

## Resonant Coupling of Ion-Cyclotron Waves to Energetic Helium Ions

K. H. Finken,<sup>1</sup> R. Koch,<sup>2</sup> H. Euringer,<sup>1</sup> G. Van Wassenhove,<sup>2</sup> J. A. Boedo,<sup>4</sup> D. S. Gray,<sup>4</sup> D. L. Hillis,<sup>3</sup>  
P. Huet,<sup>2</sup> G. Mank,<sup>1</sup> D. Van Eester,<sup>2</sup> R. Van Nieuwenhove,<sup>2,\*</sup> G. Van Oost,<sup>2</sup> and H. F. Tammen<sup>5</sup>

<sup>1</sup>*Institut für Plasmaphysik, Forschungszentrum Jülich, Association Euratom-Kernforschungsanlage, 52425 Jülich, Germany*

<sup>2</sup>*Laboratoire de Physique des Plasmas, Laboratorium voor Plasmafysica, Ecole Royale Militaire, Koninklijke Militaire School, Association Euratom-Etat Belge, Associatie Euratom-Belgische Staat, Brussels, Belgium*

<sup>3</sup>*Fusion Energy Division, Oak Ridge National Laboratory, Oak Ridge, Tennessee 37831*

<sup>4</sup>*Institute for Plasma and Fusion Research, University of California at Los Angeles, Los Angeles, California 90024*

<sup>5</sup>*FOM-Instituut voor Plasmafysica "Rijnhuizen," Association Euratom-FOM, Nieuwegein, The Netherlands*

(Received 12 October 1993)

First measurements were performed to test a model prediction which states that the off-axis coupling of ion-cyclotron waves to energetic helium ions can generate either an inward or an outward drift of these particles. Ion-cyclotron waves with a power of up to 1 MW are coupled to energetic particles at the high field side, the low field side, or in the center by varying the toroidal magnetic field. When changing the heating power or the resonance location, the variation of the concentration of the energetic helium in the plasma agrees qualitatively with the model predictions.

PACS numbers: 52.55.Pi, 28.52.Cx

In recent years, fusion research on tokamaks has made substantial progress on plasma confinement under conditions with strong auxiliary heating power. The scaling laws achieved in present-day machines promise ignition in a next step device like ITER. An open problem for the ignition remains the exhaust of the helium ash, which has to be removed on a time scale of at most 10 energy confinement times [1–5]. Experiments have been performed on the helium distribution in the plasma, the helium transport, and accumulation of helium in the divertor chamber [5–14]. Investigations with full pumping capabilities have been executed by the toroidal pump limiter ALT-II on TEXTOR [15–20]. Also, proposals were carried out to remove the helium by implantation in nickel [21]. Finally, it is also proposed to interact resonantly with the helium ions inside the plasma. First experiments on this last concept will be described in the following.

According to a proposal of Chang and co-workers [22–24] it is possible to use resonant ion-cyclotron (IC) waves interacting with the  $\alpha$  particles to expel them when they have already transferred more than 90% of their energy to the background plasma. The energy of these He ions is in the 100 keV range. A coupling of IC waves to this particle group is promising, because on one hand the requirement in heating power is not dramatic and on the other hand the resonance frequency is still sufficiently separated from that of deuterium.

The radial transport of energetic ions is a consequence of vertical drift motions induced by the gradient of the magnetic field [24]. If  $\text{grad}\mathbf{B}$  drift is upwards directed, it leads to an inward movement of the ions in the lower half of the tokamak and to an outward motion in the upper part. Under normal plasma conditions these drifts cancel, but a net effect persists if the symmetry is broken. The symmetry can be broken by off-axis, directional coupling of an IC wave to particles moving in a specified direction (here antiparallel) to the magnetic field lines

(e.g., heating on the low field side with phased antennae), as sketched in Fig. 1. If the wave couples at the periphery to the particle group moving downwards on the low field side along the magnetic field lines ( $v_0$ ), these particles gain energy; the particle group moving into the opposite direction is not influenced by the wave. At the bottom, the particle number with lower energy has decreased and the number with higher energy increased. Further on its path the heated particle group loses energy because of collisions and the lower energy group increases, leading to a top-bottom imbalance of the particle population. Together with the curvature drift ( $v_D$ ) acting on the particles this imbalance leads to the above mentioned overall drift.

The small up-down asymmetries caused by weak collisions can lead to large fluxes due to the large drift velocity of the fast particles. In a thermonuclear plasma, fast ions are fairly noncollisional; i.e.,  $v_c/\omega_T$ , the ratio of the collision frequency ( $v_c \approx 1/\tau_s$ , with  $\tau_s$  the slowing down time) to the bounce or transit frequency  $\omega_T$ , is a small

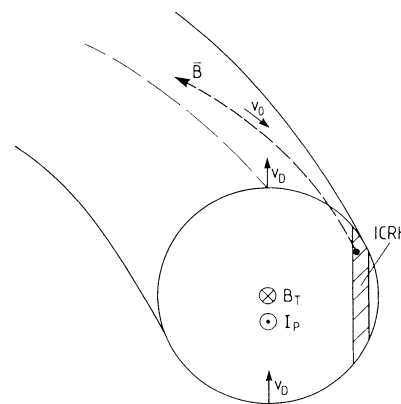


FIG. 1. Sketch of the flows inducing the helium drift.

quantity. In order to create a significant asymmetry, the RF "heating frequency"  $\nu_{RF} \approx (dE/dt_{RF})/E$  ( $E$  is the energy of the fast particle population) has to be of the same order as the collision frequency  $\nu_{RF} \approx \nu_c$ . Then the velocity perturbation  $\Delta v/v$  and the up-down asymmetry  $\Delta n/n$  are of the same order  $\nu_c/\omega_T$ . It is shown by Chang, Lee, and Weitzner [24] that in the case of ITER for  $P_{RF} \approx 20$  MW such a collisionality is sufficient to produce radial flows  $\Gamma_r \approx \Delta n v_D \approx n v_c v_D / \omega_T \approx n v_{RF} v_D / \omega_T$  of the correct order of magnitude ( $10^{20} \text{ m}^{-2} \text{ s}^{-1}$ ).

In TEXTOR, the amount of power needed to have  $\nu_{RF} \approx \nu_c$  is readily estimated using the fact that  $\nu_{RF}$  is the ratio of the RF power density and beam energy density  $\nu_{RF} = (P_{RF}/V_{RF})/(E_{beam}/V_{beam})$  with  $V_{RF}$  and  $V_{beam}$  the volumes into which the RF and the beam power are deposited. The energy in the beam component  $E_{beam}$  is the product of the average energy of a beam ion during its slowing down phase  $E_{av}$  by the number of fast ions  $(dn/dt)\tau_s$  with the number of neutrals injected per second ( $dn/dt = P_{NI}/E_0$  where  $E_0$  is the energy of a neutral beam particle). This leads to  $\nu_{RF}/\nu_c \approx (V_{beam}/V_{RF})(P_{RF}/P_{NI})(E_0/E_{av})$ , showing that  $\nu_{RF}$  is a few times  $\nu_c$  when the RF power is chosen close to  $P_{NI}$ . A simple computation using Eq. (14) of Ref. [23] shows also that the total RF induced flux is of the same order as the total particle input flux by the beam, i.e., a few times  $10^{18} \text{ particles m}^{-2} \text{ s}^{-1}$ . Finally, the total RF power cannot be much larger than the Coulomb cooling power ( $NE_{av}/\tau_s$  with  $N$  the density of the energetic ions [23]); otherwise the RF causes trapping of the fast ions and the efficiency of the RF pumping is reduced. In the TEXTOR case this power is of the order of 1 MW. These very simple estimates indicate that the mechanism proposed by Chang should be of the correct order of magnitude in TEXTOR for  $P_{NI} \approx 1$  MW (40 keV neutrals) and  $P_{RF} \leq 1$  MW.

This basic idea has been tested on TEXTOR for the first time. TEXTOR is a medium sized tokamak with the characteristic parameters  $R=1.75$  m,  $a=0.46$  m,  $I_p \leq 500$  kA, and  $B_T \leq 2.8$  T. The device is equipped with two neutral beam injectors and an ion-cyclotron heating system (ICRH) using two pairs of antennas with a maximum total power of 4 MW. The neutral beams inject nearly tangentially into the plasma; one of the beams shoots in the codirection (i.e., parallel to the plasma current) and the other one in the counterdirection. Charge exchange light ( $P_a$  line of  $^4\text{He}$ ) from beam line number I (counterinjection) is observed on ten radially distributed spectroscopic channels. The line spectrum is measured on these channels and provides a picture of the toroidal velocity distribution of the helium ions.

The coinjector (NI-II) is equipped with a cryopump. A processing of the pump with argon frost allows a pumping of helium and the generation of an energetic neutral beam [14,25]. In order to couple the IC waves to the helium only and not to the deuterium majority, the  $^3\text{He}$  isotope is chosen. The counterinjector (NI-I) provides at reduced intensity the deuterium neutrals needed

for charge exchange. NI-II produces 40 keV  $^3\text{He}$  neutrals and is switched on from 1 to 2 s after the start of the discharge. NI-I (D) operates at 50 keV and is activated between 1.5 and 2 s.

The toroidal asymmetry in the wave-particle interaction is provided by the directionality of the fast He-ion source and no asymmetric wave launch is necessary, in agreement with Chang's proposal [24]. In the experiments  $\pi$  phasing between adjacent antennas is used. To induce the drift, off-axis ICR heating is essential. The drift direction can be modified by two means: (a) inverting the plasma current and the toroidal magnetic field ( $\nabla \mathbf{B} \times \mathbf{B}$  is inverted) or (b) positioning the resonance layer either to the high field side or to the low field side of the plasma (variation of  $B_T$ ). Both schemes have been investigated, but case (b) is simpler and therefore is the only one described here. For the following experiments  $I_p$  and  $B_T$  were inverted as compared to the normal operation of TEXTOR. The drifts in the actual experimental situation are those of Fig. 1.

Figure 2, curve *a*, shows the spectral output from a central horizontal channel for the  $^3\text{He}$  beam alone and curve *b* shows that from both beams. Only the long wavelength wing of the spectral line is represented; the thermal part of the spectrum is not recorded, because its intensity is too large as compared to the high energy contribution so that it would saturate the detector. The spectral range considered corresponds to 15–50 keV comoving ions (large Doppler redshift). Because the fast He ions are injected in the codirection only, there is no corresponding blueshifted light wing at small wavelengths. The signal *a* is peaked towards the high energy end of the spectrum; i.e., one sees predominantly the high energy particles (40 keV). This is the spontaneous  $\text{He}^+$  emission light resulting from the finite lifetime of the just ionized He ions before they undergo a second ionization. The lifetime of the  $\text{He}^+$  ions amounts to 0.5–1 turn around the plasma before further ionization. During this

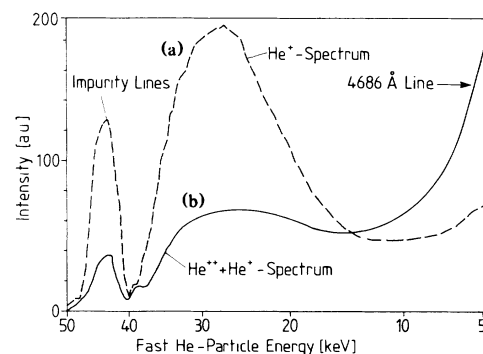


FIG. 2. Curve *a*, emission ( $t=1.1$  s), and curve *b*, emission plus charge exchange ( $t=1.6$  s) of the high energy part of the helium spectrum. The emission occurs due to the finite ionization length of the singly ionized helium after injection by the beam. The spectra are recorded by one of the horizontal optical multichannel array (OMA) channels.

time they emit the  $P_\alpha$  line, which is used for the charge exchange spectroscopy. These particles do not have enough time to slow down before they are fully ionized; the most prominent spectral feature is a peak near the injection energy, which is spreading due to the finite width of the beam and geometrical effects. Spectrum  $b$  of Fig. 2 is a superposition of the previous spontaneous emission signal  $a$  and of the charge exchange signal resulting from the emission by excited  $\text{He}^+$  ions created by charge exchange ( $\text{He}^{++} + \text{D}^0 \leftrightarrow \text{He}^+ + \text{D}^+$ ) with the slowing-down  $\text{He}^{++}$  population. The magnitude of the two signals  $a$  and  $b$  cannot directly be compared because they correspond to different densities and therefore to a different number of fast ions in the discharge [ $\propto (dn/dt)\tau_s$ ]. The flat part of spectrum  $b$  is reminiscent of a distribution function of well-confined fast ions (confinement time  $\geq \tau_s$ ). At low energy the wing of the Maxwellian distribution corresponding to the thermalized  $\text{He}^{++}$  is apparent.

Figure 3 shows the time dependence of the light, measured along a chord localized at 8 cm outboard from the toroidal axis, together with the timing of the NBI and RF pulses. The bottom curve shows a sequence of spectra of the type shown in Fig. 2, recorded by an optical multichannel array. Taking the Shafranov shift into account, this CXS channel is central. During the first part of the pulse (1–1.5 s) the diagnostic D beam is not operated and only the spontaneous emission light (curve  $a$ ) of  $\text{He}^+$  is measured. The intensity decreases with time, because the He injection causes a strong density rise and therefore an increase in the ionization rate that decreases the  $\text{He}^+$  lifetime. During the second part of the pulse (1.5–1.9 s) the D beam is activated and there is a strong increase in the light corresponding to the CXS signal. As the density continues to increase during the second part, the relative

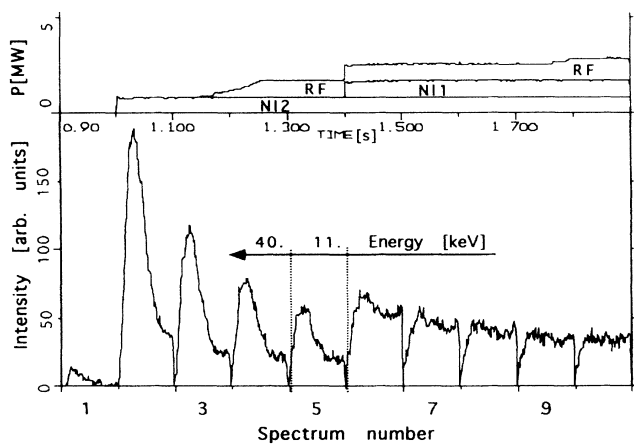


FIG. 3. Shot number 54856 with  $B_T = 1.9$  T. Bottom curve: Temporal sequence of spectra recorded by an OMA system (channel 6, line of sight 8 cm outboard of the magnetic axis). Each spectrum is sampled over a time interval of 100 ms. Top curves: Sequence of NBI and RF pulses.

contribution of the spontaneous light emission becomes smaller and smaller. It is important to note that in the absence of RF this part of the signal is independent of the value of  $B_T$ . Keeping everything else constant, the CXS signal can be varied by adding ICRH and changing the resonance position in a  $B_T$  scan. For the given TEXTOR configuration ( $B_T$  counterclockwise when seen from the top) the  $\nabla \mathbf{B} \times \mathbf{B}$  drift for the ions is directed upwards. The co-injected He ions move downwards at the low field side and upwards at the high field side. An IC wave coupling to the plasma high field side ( $B_T < 1.9$  T,  $f_{RF} = 38$  MHz,  $2\omega_{ci}$  heating) therefore should lead to an outward drift of the energetic helium and a coupling at the low field side ( $B_T > 1.9$  T) to an inward drift.

The dependence of the CXS signal intensity on  $B_T$  in the presence of RF is exhibited in Fig. 4, which shows the ratio of the spectral light intensity at different  $B_T$ 's to that in Fig. 3 (bottom). For the latter shot, the cyclotron resonance is centrally located and no pump-in/out of fast He should occur. This is actually what happens as shown by the circles (discharge without RF; ratio nearly equal to 1). With RF and different  $B_T$ 's Fig. 4 also shows the trends expected from theory. When the cyclotron layer is located at the LFS, the fast He ions are driven inward by the RF and their number increases in the center (triangles). If the cyclotron layer is moved to the HFS the converse occurs (crosses and inverted triangles). The  $B_T$  dependence of the CXS signal is in reality stronger than shown in Fig. 4 as the contribution of the spontaneous emission of the  $\text{He}^+$  was not subtracted from the signal.

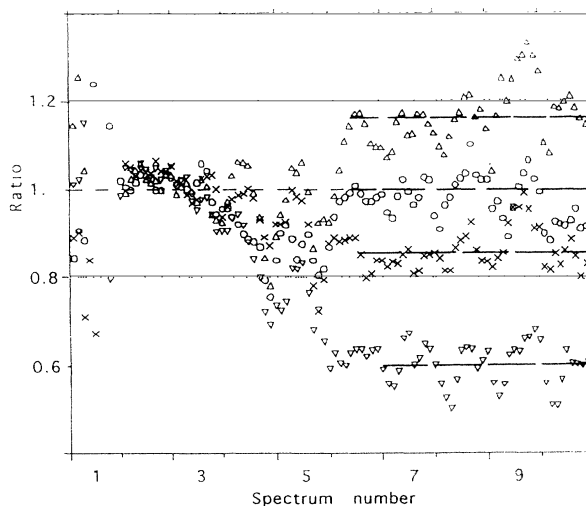


FIG. 4. Ratio of signals, similar to that of Fig. 3 (bottom), for the shots listed below, to the signal of Fig. 3. The highest energy part of the signals (sharp rise of signal in the range 31–40 keV) is not taken into account, because signal noise at small values increases the scatter of the ratio.  $\circ$ : shot number 54861, no RF,  $B_T = 2.0$  T;  $\Delta$ : shot number 54858 with RF,  $B_T = 2.1$  T;  $\times$ : shot number 54855 with RF,  $B_T = 1.8$  T;  $\nabla$ : shot number 54854 with RF,  $B_T = 1.7$  T. The dashed lines provide a guide for the eye.

Note that the spontaneous emission signal ( $t < 1$  s) is independent of the magnetic field, indicating that the shots are similar.

Because of the strong recycling of the He, the pumping effect by the RF is hard to detect (at least in an unambiguous way) in the standard diagnostics. For example, the line averaged density is nearly identical for all shots except the lowest  $B_T (\leq 1.8$  T), for which it becomes significantly larger mainly due to a broadening of the profile [the increase of the central density is 5% for shot 54855 and (15–20)% for shot number 54854]. This might be due to a stronger recycling resulting from the expulsion of the fast He by RF, but this interpretation remains speculative. Another interesting observation is that the diamagnetic energy increases with the RF; the maximum increase is observed at the lowest  $B_T (\leq 1.8$  T). This larger increase might be attributed to the central absorption of RF by the D beam at the third harmonic. The absorption at the third harmonic is predicted to be rather weak ( $\leq 10\%$ ) and does not prevent the interaction with the energetic helium ions [26].

The CXS signal behavior indicates without any doubt that the variation in the light intensity is a pure RF effect and a consequence of the variation of the  $^3\text{He}$  cyclotron layer location. Looking for an alternative explanation, the only one could be that we are observing a pure heating effect rather than a transport effect. Although the RF heating increases the perpendicular energy while the light observation is made in parallel direction, this explanation might marginally fit at higher  $B_T$  (2.1 T) where the increase in the number of fast He<sup>++</sup> ions could be attributed to off-axis heating by RF. The presence of the third harmonic D layer at  $x \approx 13$  cm might then explain some reduction of the effect at 1.9 T. However, this mechanism (with only  $\approx 10\%$  absorption per transit) cannot explain the total disappearance of the effect. Similarly no explanation based on D and/or  $^3\text{He}$  heating can explain the reduction of light intensity at  $B_T = 1.8$  and 1.7 T, especially as the heating effect is stronger in this condition (larger energy). Some reduction in the signal intensity ( $\approx 5\%$  at 1.8 T and maximum 20% at 1.7 T) results from the somewhat larger central density. But this effect cannot explain the reductions shown in Fig. 4.

Even though an active helium ash expulsion according to Chang's model seems attractive, a severe difficulty should be mentioned which is connected with this concept, if applied to a fusion reactor: If the concept works as expected, particles with energies of 100 keV leave the plasma and hit the wall. This is only possible if the particles leave the plasma at predictable, well defined positions, which can be armored. If this cannot be guaranteed, the high energy particles are more harmful than helpful. Nevertheless possible scenarios for helium removal should be studied thoroughly, because this problem is critical for a fusion reactor.

We wish to thank C. S. Chang for discussions and to

express our gratitude to the TEXTOR group, in particular to B. Giesen, P. Hüttemann (TEXTOR operation), M. Lochter, R. Uhlemann, H. Reimer (neutral beams), F. Durodié (ICRH), and M. Korten (data acquisition).

\*Researcher at the NFSR, Brussels, Belgium.

- [1] D. Reiter, G. H. Wolf, and H. Keuer, Nucl. Fusion **30**, 2141 (1990).
- [2] D. Reiter *et al.*, Plasma Phys. Controlled Fusion **33**, 1579 (1991).
- [3] D. Reiter, G. H. Wolf, and H. Keuer, J. Nucl. Mater. **176-177**, 756 (1990).
- [4] M. Kaufmann *et al.*, Nucl. Fusion **25**, 89 (1985).
- [5] M. H. Redi *et al.*, Nucl. Fusion **32**, 1689 (1991).
- [6] M. Shimada *et al.*, Phys. Rev. Lett. **47**, 796 (1981).
- [7] J. C. De Boo *et al.*, Nucl. Fusion Lett. **22**, 572 (1982).
- [8] R. J. Fonck and R. A. Hulse, Phys. Rev. Lett. **52**, 530 (1984).
- [9] E. J. Synakowski *et al.*, Phys. Rev. Lett. **65**, 2255 (1990).
- [10] D. L. Horton *et al.*, in *Proceedings of the 14th International Conference on Plasma Physics and Controlled Fusion Research, Würzburg, 1992* (International Atomic Energy Agency, Vienna, 1993).
- [11] T. Sugie *et al.*, in *Proceedings of the 14th International Conference on Plasma Physics and Controlled Fusion Research* (Ref. [10]).
- [12] R. Décoste *et al.*, in *Proceedings of the 20th EPS Conference on Controlled Fusion and Plasma Physics* (European Physical Society, Genève, 1993), Vol. 17C, p. 295.
- [13] M. R. Wade *et al.*, in *Proceedings of the 20th EPS Conference on Controlled Fusion and Plasma Physics* (Ref. [12]), Vol. 17C, p. 63.
- [14] A. Sakasai *et al.*, in *Proceedings of the 20th EPS Conference on Controlled Fusion and Plasma Physics* (Ref. [12]), Vol. 17C, p. 67.
- [15] K. H. Finken *et al.*, J. Nucl. Mater. **176-177**, 816 (1990).
- [16] D. L. Hillis *et al.*, Phys. Rev. Lett. **65**, 2382 (1990).
- [17] D. L. Hillis *et al.*, J. Nucl. Mater. **196-198**, 35 (1992).
- [18] D. L. Hillis *et al.*, in *Proceedings of the 13th International Conference on Plasma Physics and Controlled Fusion Research, Washington D.C., 1990* (International Atomic Energy Agency, Vienna, 1991).
- [19] U. Samm *et al.*, J. Nucl. Mater. **196-198**, 633 (1992).
- [20] R. R. Weynants *et al.*, in *Proceedings of the 14th International Conference on Plasma Physics and Controlled Fusion Research* (Ref. [10]).
- [21] J. N. Brooks *et al.*, J. Nucl. Mater. **196-198**, 664 (1992).
- [22] C. S. Chang and P. Colestock, Phys. Fluids B **2**, 310 (1990).
- [23] C. S. Chang, Phys. Fluids B **3**, 259 (1991).
- [24] C. S. Chang, J.-Y. Lee, and H. Weitzner, Phys. Fluids B **3**, 3429 (1991).
- [25] H. B. Reimer *et al.*, in *Proceedings of the 16th Symposium on Fusion Technology, London, 1990* (Elsevier, Amsterdam, 1991), p. 1191.
- [26] G. Van Wassenhove *et al.*, in *Proceedings of the Europhysics Topical Conference on Radio-Frequency Heating and Current Drive of Fusion Devices*, Europhysics Conference Abstracts, 1992 (Ref. [12]), Vol. 16E, p. 141.